Available online at www.sciencedirect.com

ScienceDirect

Ceramics International 40 (2014) 7889–7897

CERAMICS INTERNATIONAL

www.elsevier.com/locate/ceramint

Controlling surface microstructure of calcium phosphate ceramic from random to custom-design

Liao Wang[a], Xiaoman Luo[b], Davide Barbieri[b], Chongyun Bao[a,*], Huipin Yuan[b,c,**]

[a]State Key Laboratory of Oral Diseases, West China Hospital of Stomatology, Sichuan University, Chengdu 610041, China
[b]Xpand Biotechnology BV, Prof. Bronkhorstlaan 10, bld 48, 3723MB Bilthoven, The Netherlands
[c]Tissue Regeneration Department, Twente University, Drienerlolaan 5; 7522 NB Enschede, The Netherlands

Available online 2 January 2014

Abstract

Calcium phosphate ceramics have long been studied as bone graft substitutes due to their similarity with the mineral constitute of bone and teeth, excellent biocompatibility and bioactivity. Chemical composition, macrostructure and surface microstructure are believed to be important for the bone formation within calcium phosphate ceramics. Surface microstructure has shown its crucial role in the osteogenic response of calcium phosphate ceramics; however the presence of surface irregularities and random distribution of surface microstructure in traditional calcium phosphate ceramics make it difficult to explain how surface microstructure play its role in bone formation. In the present study, we evaluated the influence of various starting apatites and sintering temperatures on the surface microstructure of the resulting hydroxyapatite ceramics. In order to minimize the randomness of the surface microstructure, laser ablation was used to generate custom-designed surface microstructures. The resulting hydroxyapatite ceramics with controlled surface microstructures would be helpful to study the role of surface microstructure on bone formation and may provide useful information for further optimization of calcium phosphate ceramics for bone regeneration.

Keywords: A. Powders: chemical preparation; A. Sintering; B. Microstructure-final; E. Biomedical applications

1. Introduction

Bone defect can result from tumor resection, trauma, disease and congenital anomalies. When a bone defect is too large to heal by itself, the so called critical-sized defect, it requires bone graft materials [1,2]. To this end, several grafting materials have been considered, including autograft, allograft, xenograft and synthetics. Autograft has long been considered as the "Gold Standard" in bone repair because of its excellent osteoconductive and osteogenic properties, high biocompatibility and immunological safety. However, the necessity of a second surgical procedure may lead to undesired scarring, long healing time, morbidity and pain, limiting its use. Allograft and xenograft could be alternatives to autograft, but they have less bone regeneration potential and may cause immunological rejection. Synthetics do not have such problems and could be ideally optimized with respect to biocompatibility, osteoconductive property and resorption rate by controlling their chemical composition, macro and microporosity, etc.

Among synthetic materials, calcium phosphate ceramics have been extensively evaluated as bone grafts due to their chemical similarity to bone minerals, excellent biocompatibility, osteoconductive and bioactivity properties [3,4]. Moreover, calcium phosphate ceramics with specific physico-chemical properties could induce ectopic bone formation, thus are osteoinductive. Although this phenomenon has been shown in different animal models, such as baboon [5], monkey [6], goat [7,8], sheep [9,10], dog [11–15], rabbit [16,17], and mouse [17–19], the exact physico-chemical parameters governing the successful ectopic bone formation are not fully understood. It is believed that the osteoinductive capacity can be modulated by controlling the crystal size, crystallinity, Ca/P ratio, macroporosity and microporosity. Recently an increasing number

*Corresponding author at: State Key Laboratory of Oral Diseases, West China Hospital of Stomatology, Sichuan University, Chengdu 610041, China.
**Corresponding author at: Xpand Biotechnology BV, Prof. Bronkhorstlaan 10, bld 48, 3723MB Bilthoven, and Tissue Regeneration Department, Twente University, Drienerlolaan 5; 7522 NB Enschede, The Netherlands.
E-mail addresses: cybao9933@scu.edu.cn, cybao9933@yahoo.com.cn (C. Bao), h.yuan@tnw.utwente.nl (H. Yuan).

0272-8842/$ - see front matter © 2014 Elsevier Ltd and Techna Group S.r.l. All rights reserved.
http://dx.doi.org/10.1016/j.ceramint.2013.12.136

of studies have illustrated that the micropores might be an important determinant of osteoinduction [6,7,20,21]. It has been suggested that micropores could increase the surface area of calcium phosphate ceramics, which facilitated ion exchange and bone-like apatite formation. This could be accompanied by the binding of endogenous bone inducing proteins to the surface from body fluids (i.e. growth factors like bone morphogenetic proteins). All of these events may, in turn, facilitate the recruitment and homing of relevant pluripotent stem cells (i.e. bone marrow mesenchymal stem cells) to form new bone in ectopic sites [22].

At the cellular level, the substratum interface functions as more than a simple definition boundary between the host and implanted devices; instead, it presents primary cues for cellular adhesion and subsequent induction of tissue integration, which play crucial roles in tissue regeneration [23,24]. As the functions of the extracellular environment have been explored for years, the surface microstructure has been proved to have complex interactions with cells [25–36]. The ability of the substrate topography to influence cell behaviors was first noted by Harrison in 1911 when he cultured cells on a spider web. It was observed that cells followed the fibers of the web in a phenomenon called physical guidance or stereotropism [37]. Later, in 1964, it was first proposed that cells react to the topography, or to their surrounding environment, in the process of "contact guidance" [38]. Thanks to the development of various micro and nanostructure fabrication techniques, a large number of research groups have devoted their attentions to this emerging area. In the last decade, the interest in basic knowledge of cell–substrate interactions has increasingly grown, and it has now been recognized that the microstructure plays a key role in causing the differences observed in cell′s behavior both in vitro and in vivo [25,26]. Studies on the interactions between various substrate microstructures and cells have included a wide variety of cell types such as endothelial cell, fibroblasts, leukocytes, chondrocytes, osteocytes, oligodendrocytes, smooth muscle cells and mesenchymal stem cells. In these studies, it has been recognized that these cells strongly react to microstructures, which modulated their adhesion, alignment, migration, morphology, proliferation, vitality and differentiation [25–36]. More specifically, it was demonstrated that the use of nanoscale surface disorder could stimulate human mesenchymal stem cells (MSCs) to produce bone mineral in vitro, in the absence of osteogenic supplements. The same study also proved that this approach has similar efficiency to others where cells were cultured in osteogenic media [35].

Concluding, the substrate topography may induce osteogenic differentiation of mesenchymal stem cells via not only specific protein adsorption but also via the specific surface topography created by the micropores on the surface of materials. In respect of this, a calcium phosphate material with proper surface microstructure should be carefully designed to distinguish the roles of protein adsorption and surface topography in instructing cells.

Careful surface structure designs have been applied on different materials with various methods [25,26]. However, a well-controlled surface microstructure or nanostructure on calcium phosphate ceramics has not been reported so far. Because of the intrinsic brittleness of calcium phosphate ceramics, it is difficult to precisely control the surface structure with conventional methods (e.g. surface roughening or plasma spraying). Laser ablation has high potential for micromachining of various materials, and this method was increasingly proved to be a promising tool for 3D micro-texturing of material′s surfaces. The advantages of laser structuring include its very high fabrication rate, high resolution, non-contact interaction, applicability for many types of substrate and reproducibility. Furthermore, lasers can be easily incorporated with computer-assisted fabrication systems for complex and customized 3D matrix structure design and manufacture [39,40].

In this study, we first synthesized hydroxyapatite ceramics with random and irregular surface microstructures by controlling the particle size and distribution of the starting apatites and sintering temperatures. We then used laser ablation method in order to get custom designed surface microstructures of the synthesized ceramics.

2. Material and methods

2.1. Starting apatites and characterization

Two apatite slurries with a Ca/P molar ratio of 1.67 were prepared with either concentrated or diluted starting chemicals. Both apatite slurries were synthesized by mixing $Ca(NO_3)_2 \cdot 4H_2O$ (Fluka) with $(NH_4)_2HPO_4$ (Fluka). In general, $Ca(NO_3)_2 \cdot 4H_2O$ solution was kept stirring at 500 rpm at 80 °C and $(NH_4)_2HPO_4$ solution was added to it. Ammonium hydroxide solution was added as well to keep the pH of the slurry above 10. After additions were terminated, stirring was kept for 2 h at 80 °C. In the case of concentrated starting chemicals, 12 mol/L ammonium hydroxide solution was added to 2 mol/L $Ca(NO_3)_2 \cdot 4H_2O$ solution at the speed of 35 mL/min, while a 2.4 mol/L $(NH_4)_2HPO_4$ solution was added at 30 mL/min. In the diluted counterparts, 3 mol/L ammonium hydroxide solution was added into $Ca(NO_3)_2 \cdot 4H_2O$ solution (0.5 mol/L) at a speed of 17.5 mL/min, then $(NH_4)_2HPO_4$ solution (0.60 mol/L) was added at the speed of 12.5 mL/min.

The two slurries were then aged at room temperature overnight, and then the supernatant was refreshed with demineralized water to remove ammonia. The slurries were then vacuum-filtered to obtain cakes. Half of the apatite cake obtained from the concentrated hydroxyapatite slurry (SCHA) were dried at 80 °C and reduced to powder using a grinder (ZM100, Retsch, Germany) with a 250 μm sieve to get apatite powder (PHA). The second half of the cake from SCHA and the one from diluted hydroxyapatite slurry (SDHA), were dried at room temperature till a water content of 20% (w/w), and stored in air-tight containers.

The chemistry of apatites from both concentrated starting chemicals and diluted chemicals were analyzed with X-ray diffraction (XRD, Miniflex, Rigaku, Japan) after sintering them at above 1000 °C for 2 h using a sintering oven (Nabertherm, Germany).

Meanwhile unsintered 800 ± 10 mg PHA powder, 1000 ± 10 mg SCHA and 1000 ± 10 mg SDHA slurry were suspended in 50 mL demineralized water respectively and viewed with light microscope (Nikon, Japan) for an overview of particle distribution. For the determination of particle size, the dried particles were gold-sputtered and analyzed with scanning electron microscope (XL30 ESEM FEG, Philips, The Netherlands) and images were analyzed in terms of the length and width of each particles.

2.2. Calcium phosphate ceramic discs and characterization

Green compact discs were made from the three apatites using a uniaxial press at 200 MPa for 5 min in a cylindrical steel mold (∅=13 mm). PHA was homogenously mixed with water at a ratio of 80% PHA to 20% demineralized water by weight, and then 350 ± 10 mg of the mixture was used to manufacture one disc. To fabricate one disc from the slurry cakes, 350 ± 10 mg of SCHA or SDHA slurry was used. Green compact discs were dried at room temperature and sintered at 700 °C, 1000 °C and 1300 °C in air. The sintering profile was as follows: the temperature was gradually increased from room temperature to the target sintering temperature in 600 min, which was kept for 480 min and thereafter it was cooled in 600 min to room temperature.

The porosity of the sintered compact discs were measured by Archimedes′ method in distilled water (n=5). More specifically, after the discs had been vacuum-dried at 50 °C for 48 h, their dry weight was recorded as m1. The samples were then immersed in water under vacuum to force the liquid into the pores of the discs until no bubbles emerged from the discs. Then, the samples were reweighed in water to produce the measurement m3. After that, the discs were carefully removed from the beaker and surface saturated water droplets were dabbed off. They were quickly reweighed in air to produce the measurement m2. The porosity of the open pores in the scaffold can then be calculated via the following formula:

$$\text{Porosity} = (m2 - m1)/(m2 - m3) \times 100\%$$

Five samples were tested to calculate the average porosity [41]. Surface morphological observations of sintered ceramics were done using scanning electron microscope (XL30 ESEM FEG, Philips, The Netherlands). Moreover, to confirm the porosity of the discs, specific discs minimize the random micropores were subjected to Brunauer–Emmett–Teller (BET) Surface Area Analysis regarding specific surface area.

2.3. Manufacture of topography using laser

According to the results of SEM, the most appropriate sintered apatite discs were selected for microstructure modification. The laser ablation was performed on discs using Rega9000 Ti:Sapphire Regenerative Amplifier with a radiation wavelength of 800 nm and pulse repetition rate of 250 kHz. Designed patterns were line-, pore-, triangle-, grid- and pore-like, and the size of each patterns were controlled by the variation of the diameters of laser beam. Finally the custom-designed surface microstructures on calcium phosphate ceramics were analyzed with scanning electron microscope (XL30 ESEM FEG, Philips, The Netherlands).

3. Results

3.1. Characterization of the starting apatites

The XRD spectra were in good agreement with that of the standard hydroxyapatite (Fig. 1), indicating that the concentration of starting chemicals does not have influence on the chemistry of the resulting apatite.

The size of apatite particles in the slurry was affected by the concentration of the starting chemicals (Fig. 2). Homogenous and smaller apatite particles were observed within apatite slurry obtained in the case of diluted starting chemicals (SDHA, Fig. 2C and c), while larger apatite particles were noted in the slurry prepared with the concentrated starting chemicals (SCHA, Fig. 2B and b). Inhomogeneous and even larger apatite particles or aggregates were seen in apatite powder (PHA, Fig. 2A and a).

The morphology and size of the particles were characterized with SEM (Fig. 3, Table 1). The particles in PHA and SCHA had micro-scaled dimensions with irregular shape. However, PHA group showed particles with broader range of size distribution and larger dimensions than SCHA. The particles in SDHA were nano- and submicro-scaled, with more uniform particle size distribution than SCHA and PHA.

3.2. Sintering behavior of samples

The surface topography of ceramic discs sintered at different temperature is displayed in Fig. 4. It may be observed that the surface became smoother with the increase of sintering temperature. At the temperature of 700 °C the surface in all the three groups was irregular with a lot of pores. Larger pores were seen in PHA and SCHA groups compared to SDHA. After sintering at 1000 °C, a lot of micropores randomly distributed with random dimension were present in PHA group, but few micropores were seen in SCHA group. Conversely, no micropores were observed in SDHA group.

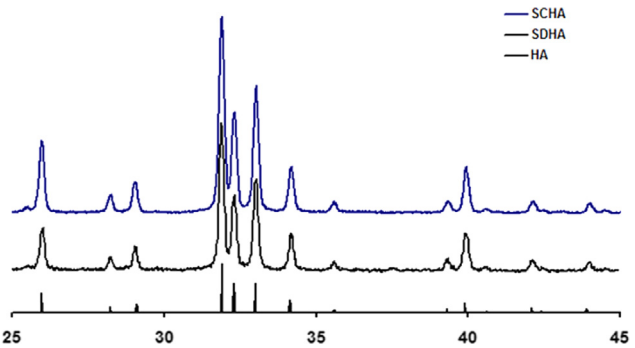

Fig. 1. XRD patterns of apatites obtained from concentrated starting chemicals (SCHA) and diluted starting chemicals (SDHA), as compared to stardard hydroxyapatite (HA).

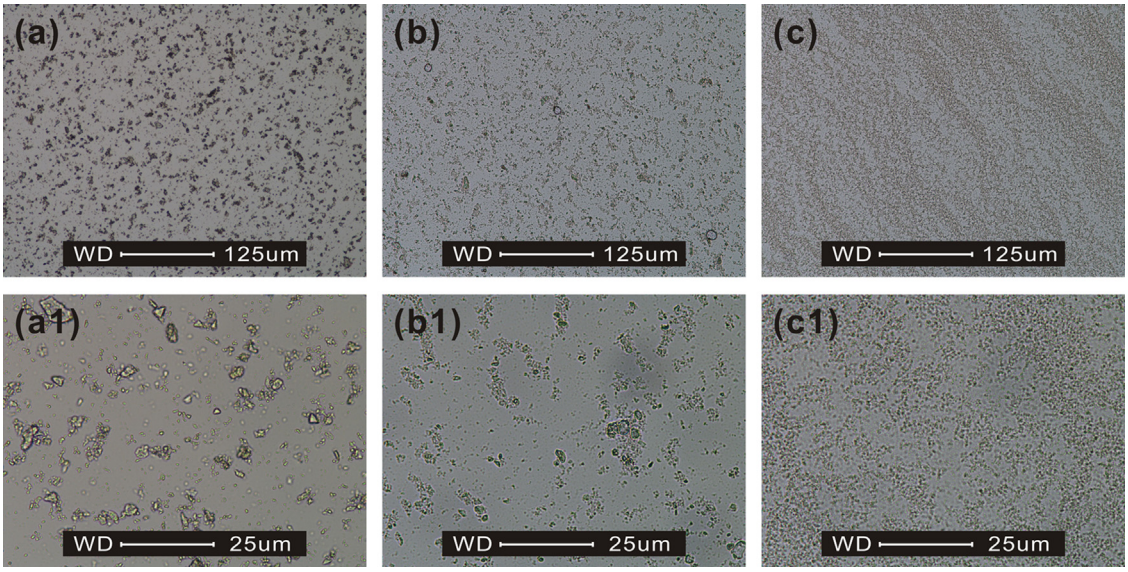

Fig. 2. Apatite particles observed with light microscope ((A and a): PHA; (B and b): SCHA; (C and c): SDHA). Magnification in (A–C) 40 × ; in (a–c) 100 × .

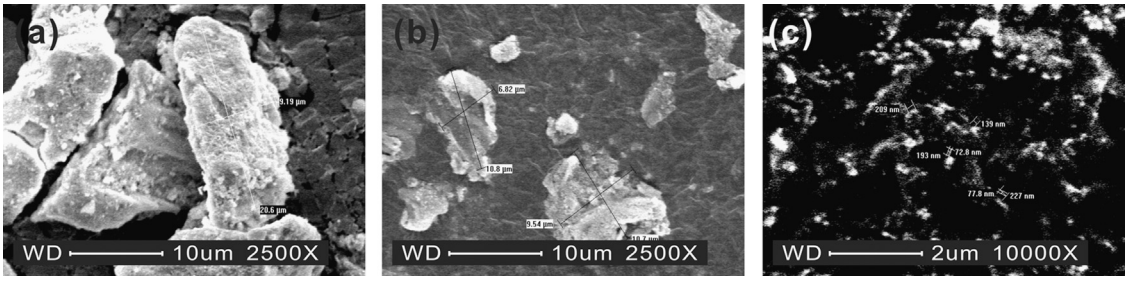

Fig. 3. Apatite particle shape and size under SEM ((A): PHA; (B): SCHA; (C): SDHA).

Table 1
Particle sizes of the starting apatites.

Sample	*Length* (μm)	*Width* (μm)
PHA	21.77 ± 8.94	11.74 ± 3.84
SCHA	8.40 ± 3.49	6.89 ± 3.99
SDHA	184.35 ± 59.85	69.00 ± 16.40

At 1300 °C, the hydroxyapatite ceramic grains became larger in all the three groups, while the pores disappeared.

The influence of the starting apatite and sintering temperature on the densification was also shown in the porosity of the discs (Table 2). Clearly, both the starting apatite and sintering temperature had influence on the porosity of the ceramics discs. In general, the porosity of each ceramic decreased with the increasing sintering temperature. However there were little difference of the porosity of SDHA sintered at 1000 °C and 1300 °C.

3.3. Laser induced micro-topography on HA samples

The porosity data (Table 2) indicated that most pores were eliminated in SDHA sintered at 1000 °C and 1300 °C and SCHA sintered at 1300 °C. However as shown in Fig. 4, the grain size in the ceramic discs sintered at 1300 °C was much larger than those sintered at 1000 °C. In order to fabricate micro-scale surface structure and make sure the bioactivity of the sintered ceramics, SDHA discs sintered at 1000 °C were selected as the substrates for laser ablation because their small grains as well as the smooth surface could reduce the impact of high sintering temperature (1300 °C) on the bioactivity of ceramics to a minimum state. To confirm the porosity, the discs were subjected to BET analysis. The specific surface area was lower than 0.001 m^2/g, demonstrating the absence of abundant random pores. After the laser ablation, different topographies with varied shape and size have been manufactured on the HA pellet discs (Fig. 5). The surface structures were precisely controlled at micron-scale.

4. Discussion

In order to design customized surface microstructures of calcium phosphate ceramics, the random microstructure of such ceramics should be avoided. To eliminate it from discs, the particle size and homogeneity of hydroxyapatite were investigated as a function of the manufacturing parameters (i.e. starting chemical concentration, initial state of apatite and sintering temperature). Afterwards, various customized surface microstructures were obtained with laser ablation.

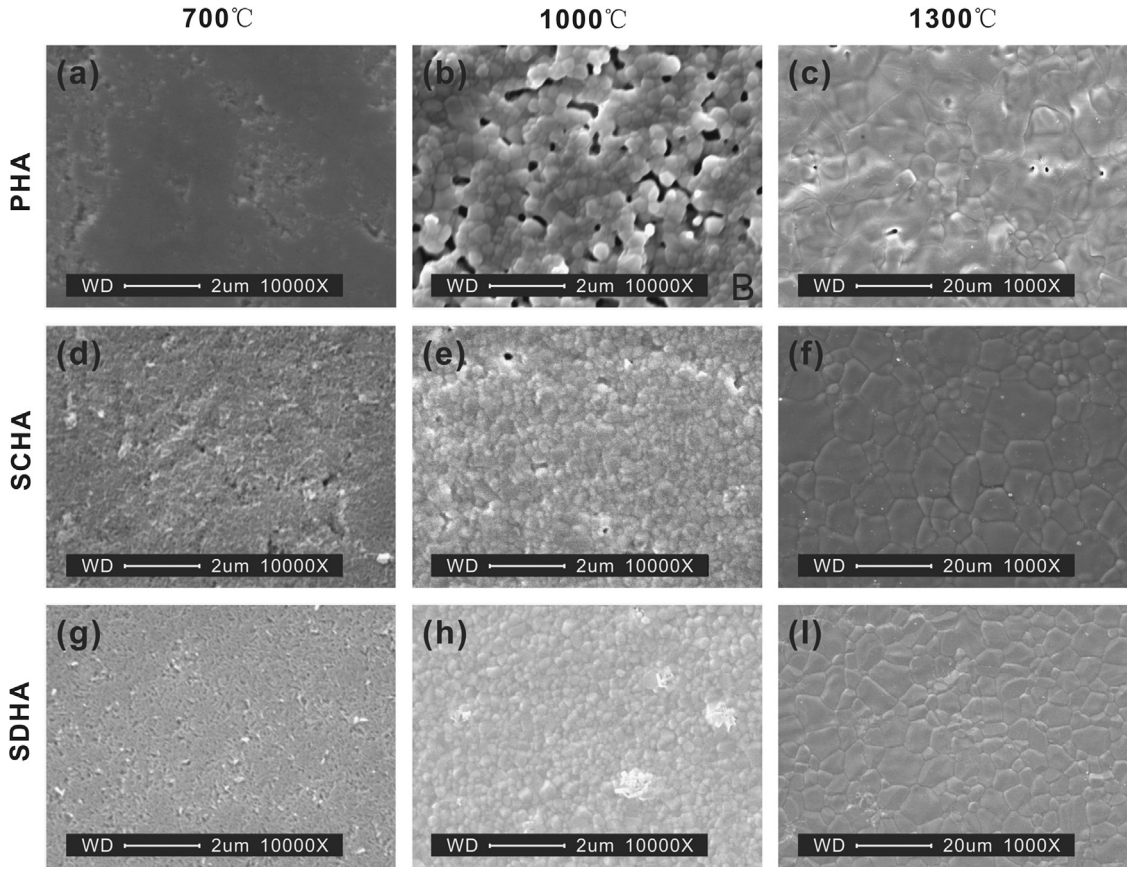

Fig. 4. Surface topographies of ceramic discs sintered at different temperatures.

Table 2
The porosity of discs at different sintering temperature (%).

Sample	*700* °C	*1000* °C	*1300* °C
PHA	28 ± 4	17 ± 2	10 ± 2
SCHA	22 ± 5	10 ± 1	7 ± 1
SDHA	19 ± 3	7 ± 1	6 ± 1

The packing of particles in ceramic processing has been studied for many years and it has been recognized to have a significant effect on the shrinkage and bulk density of ceramics during sintering as well as on other properties of the final products. Many parameters have been proved to affect the packing density of particles, such as particle size, particle size distribution, particle shape, interparticle friction, surface chemistry, agglomeration and vibration [42–46]. Among these parameters, the particle size and distribution are probably the most significant factors affecting the packing density, which in turn influences the final density of the sintered ceramics.

A number of techniques have been developed and used to synthesize hydroxyapatite, including the solid-state reactions, mechanochemical synthesis, sol–gel synthesis, hydrothermal reactions, hydrolysis, micro-emulsion syntheses, conventional chemical precipitation, combustion method and pyrolysis process or combination of two or more methods mentioned above [47]. Each of them depends on the use of special instruments and synthesis protocols, therefore the geometry of particles, particle size, particle size distribution, phase purity and crystallinity and particle agglomeration varies. Although the chemical precipitation from aqueous solutions to obtain HA depends on several variables, it is still a versatile and economic route for the synthesis of phase pure HA [47–50]. The phase-pure HA with desired particle properties could be prepared by adjusting the reaction rate, reaction PH, temperature, stirring speed as well as the aging time [51,52]. The influence of the concentration of starting chemicals on the properties of hydroxyapatite particles has been extensively studied. Generally speaking, when the temperature, stirring speed and pH are appropriate and remain constant, the diluted starting chemicals would result in a more adequate reaction of each component than the concentrated counterpart, resulting in good crystallinity with a minimal formation of particle agglomeration. The XRD results confirmed that both the SCHA and SDHA were phase-pure HA (Fig. 1). Fig. 2 and Table 1 confirmed that the use of diluted starting chemicals resulted in a uniform nanoscale hydroxyapatite grains with narrower size distribution. Conversely, microscaled particles with relatively broader size distribution were synthesized when using the concentrated starting chemicals. As regards PHA, the particle size and the agglomeration were found to be the largest, which can be explained not only by the use of concentrated staring chemicals but also with the possible agglomeration of particles during the drying process. In addition, the grinding

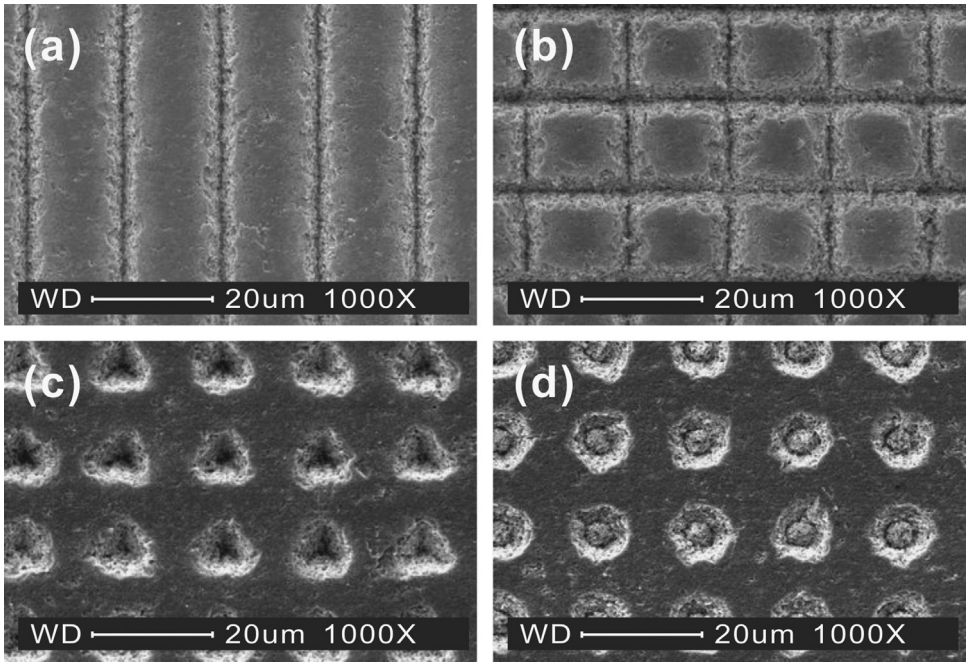

Fig. 5. Custom-designed surface microstructures on calcium phosphate ceramics with laser ablation ((A): line; (B): grid; (C): triangle; (D): pore-like).

procedure may have made the distribution of particles more inhomogenous.

The sintering kinetics of hydroxyapatite is crucial since it allows the design of ceramics with controlled grain growth, microstructure and mechanical properties. In the current study, to diminish the effect of random structures and micropores on the sintered disc, it was important to increase the density of the sintered ceramics. The sintering theories indicate that the densification of ceramic particles can result from different mechanisms, which can be divided into three categories [50]. Superficial diffusion and gaseous phase transport generally lead to a reduction of surface area without densification of the materials, the ceramics of each groups after sintered at 700 °C confirmed that there were lots of pores on the surface (Fig. 4) and the porosity (Table 2) was the highest among the three sintering temperatures. In contrast, when the sintering temperature was higher than the critical temperature (i.e. 750 °C), volume diffusion or grain boundaries diffusion occurs, which induce a reduction of surface accompanied with an increase of the apparent density, this phenomenon was confirmed by the increase of surface smoothness and decrease of porosity when the temperature was 1000 °C (Table 2). Finally when the sintering temperature was high enough (1300 °C), it will leave a nearly fully dense ceramic [50,53,54].

Some strategies have been used to improve the sintering behavior and promote the densification of HA by adding some additives in the powder, modifying the sintering conditions (e.g. temperature, pressure and time) and using other sintering techniques (e.g. liquid-phase sintering, microwave sintering and pressureless sintering combined with hot isostatic pressing (HIP)) [49,54,55]. Several additives have been used to enhance the sinterization and the stability of HA to improve its mechanical properties and bioactivity. However, there are not generally accepted additives which can effectively improve the sintering performance of HA [55–57]. Previous studies have demonstrated that the starting densification depends on the chemical composition of the precursor powder, i.e. the Ca/P ratio. Further, the final density of the sintered bodies mainly depends on the homogeneity and the particle size of the precursor powder [57]. In our study, XRD patterns demonstrated that the three starting particles were phase-pure HA, indicating they had the same Ca/P ratio. However, the particle size and distribution varied among these groups. The starting powder size of SCHA and PHA were microscaled and both of them had broad particle size distributions, while SDHA had particle size in the nanometer-scale with a uniform distribution. So the sintering behavior most likely depended on the characteristics of the starting particles. The smaller size with uniform distribution of HA particles increased the packing density resulting in reduction of the porosity of the final ceramics after sintering. This theory has been proved by the SEM results as well as by the porosity measurements (Fig. 4 and Table 2). At 700 °C, the surface topography of all samples did not change much. The arrangement of the powders was irregular, with dispersed gaps and pores on the surface. A relatively high porosity existed in each group, especially in SCHA and PHA. At 1000 °C the surface of all the samples looked regular (Fig. 4). The collapse of the large agglomerates could be observed, along with the decrease of pore size on the surface. Among the three groups SCHA presented smoother surfaces than PHA, which may be explained by its smaller particle size and more regular distribution of the particles. However owing to the nanoscale particle size and more uniform distribution, the sintered SDHA disc was the smoothest with

rare pores and gaps. Further, it was observed that the porosity of this group decreased significantly. In particular, it was seen that the porosity levels between SDHA sintered at 1000 °C and 1300 °C were not significantly different. At 1300 °C the surface of all samples looked very smooth indicating that the grain boundaries diffusion happened, and the grain size grew significantly. All of the three samples, when sintered at 1300 °C, no significant difference has been observed. In addition, the porosity of each ceramics at this sintered temperature was lowest.

In the current study, with the rise of sintering temperature from 700 °C to 1300 °C, the porosity of sintered discs decreased gradually in PHA and SCHA groups, with the porosity of SCHA lower than PHA ceramics for each sintering temperature. Although the porosity decreased with the increase of the sintering temperature, no significant differences were seen when SDHA was sintered at 1000 °C and 1300 °C which illustrated that the densification degree of SDHA was already sufficient at the sintering temperature of 1000 °C. These results can be explained with the particle size as well as the size distribution of each starting particles. More precisely, when the particle size was relatively large and the distribution was not very uniform, the packing density would be lower than the smaller particles with uniform distribution which in turn affected the final porosity and density of ceramic discs. In addition, when the particle size was small enough (i.e. at the nanometer scale) with a uniform size distribution, a relative low temperature can make the ceramics reaching the desired density and eliminating the pores.

Surface modification of HA is an important part of the processing of biomaterials to obtain enhanced mechanical properties, remodeling interactions, and bone healing [58]. The sintering temperature is believed to be an important determinant to affect the bioactivity of calcium phosphate ceramics. When the temperature is higher than 1200 °C the bioactivity of ceramics would be in worse as a consequence of grain growth and the disappearance of microporous structures. To avoid this, we chose the relatively smooth surface of SDHA obtained at the sintering temperature of 1000 °C and prepared various microstructures on the discs. In this way we could make sure that the sole determinant of the properties of the material was limited to the variation of topography. Laser ablation has high potential for micromachining of a variety of materials, and this method was demonstrated to be a promising tool for 3D micro-texturing of material′s surfaces without the alteration of the nature of the target material [56,57]. In the work of Queiroz et al., HA surface modification was performed using an excimer laser with a 248 nm radiation wavelength and 30 ns pulse duration. By modulating the laser pulse and influence of radiation, different surface topographies could be made [59]. In the current study, the diverse microstructures with different shape and size were prepared on the HA disc by incorporating with computer-assisted fabrication systems and controlling of the diameter of laser beam and energy, with these method we can further study the interactions between surface topography of material and clarify the roles of microstructure on the bone regeneration.

5. Conclusions

The influence of the reaction parameters on hydroxyapatite particle size were shown in the current study. The influence of particle size distribution and sintering temperature on the density of the final hydroxyapatite ceramics were studied as well. By controlling the concentration of starting chemicals, state of hydroxyapatite and sintering temperature, random micropores could be depleted from hydroxyapatite ceramics to allow custom design of surface microstructures. Moreover, as shown in the present study, such surface microstructures could be obtained with laser ablation. It is expected that the custom-designed surface microstructures could be useful in exploring the roles of such surface microstructures in their unique biological responses.

Acknowledgments

This work was supported by the National Natural Science Foundation of China (81371181 and 81171005) and the Doctoral Scientific Fund Project of the Ministry of Education of China (20100181110058).

Reference

[1] R. Comesaña, F. Lusquiños, J. del Val, T. Malot, M. López-Álvarez, A. Riveiro, F. Quintero, M. Boutinguiza, P. Aubry, A. De Carlos, J. Pou, Calcium phosphate grafts produced by rapid prototyping based on laser cladding, J. Eur. Ceram. Soc. 31 (1–2) (2011) 29–41.

[2] D. Alves Cardoso, J.A. Jansen, S.C. Leeuwenburgh, Synthesis and application of nanostructured calcium phosphate ceramics for bone regeneration,, J. Biomed. materials Res. Part B Appl., Biomater. 100 (8) (2012) 2316–2326.

[3] D. Grossin, S. Rollin-Martinet, C. Estournes, F. Rossignol, E. Champion, C. Combes, C. Rey, C. Geoffroy, C. Drouet, Biomimetic apatite sintered at very low temperature by spark plasma sintering: physico-chemistry and microstructure aspects, Acta Biomater. 6 (2) (2010) 577–585.

[4] S. Ramesh, C. Tan, S. Bhaduri, W. Teng, I. Sopyan, Densification behaviour of nanocrystalline hydroxyapatite bioceramics, J. Mater. Process. Technol. 206 (1) (2008) 221–230.

[5] U. Ripamonti, The morphogenesis of bone in replicas of porous hydroxyapatite obtained from conversion of calcium carbonate exoskeletons of coral,, J. Bone Joint Surg. Am. 73 (5) (1991) 692–703.

[6] U. Ripamonti, Osteoinduction in porous hydroxyapatite implanted in heterotopic sites of different animal models, Biomaterials 17 (1) (1996) 31–35.

[7] P. Habibovic, H. Yuan, C.M. van der Valk, G. Meijer, C.A. van Blitterswijk, K. de Groot, 3D microenvironment as essential element for osteoinduction by biomaterials, Biomaterials 26 (17) (2005) 3565–3575.

[8] E.W. Bodde, C.T. Cammaert, J.G. Wolke, P.H. Spauwen, J.A. Jansen, Investigation as to the osteoinductivity of macroporous calcium phosphate cement in goats, J. Biomed. Mater. Res. Part B: Appl. Biomater. 83 (1) (2007) 161–168.

[9] A.K. Gosain, L. Song, P. Riordan, M.T. Amarante, P.G. Nagy, C.R. Wilson, J.M. Toth, J.L. Ricci, A 1-year study of osteoinduction in hydroxyapatite-derived biomaterials in an adult sheep model: Part I, Plast. Reconstr. Surg. 109 (2) (2002) 619–630.

[10] H. Yuan, H. Fernandes, P. Habibovic, J. de Boer, A.M. Barradas, A. de Ruiter, W.R. Walsh, C.A. van Blitterswijk, J.D. de Bruijn, Osteoinductive ceramics as a synthetic alternative to autologous bone grafting, Proc. Natl. Acad. Sci. 107 (31) (2010) 13614–13619.

[11] Z. Xingdong, Z. Pin, Z. Jianguo, C. Weiqun, C. Wu, A study of hydroxyapatite ceramics and its osteogenesis, in: A. Ravaglioli, A. Krajewski (Eds.), Bioceramics and the Human Body, Springer, Netherlands, 1992, pp. 408–416.
[12] C. Klein, K. de Groot, W. Chen, Y. Li, X. Zhang, Osseous substance formation induced in porous calcium phosphate ceramics in soft tissues, Biomaterials 15 (1) (1994) 31–34.
[13] N. Kondo, A. Ogose, K. Tokunaga, H. Umezu, K. Arai, N. Kudo, M. Hoshino, H. Inoue, H. Irie, K. Kuroda, Osteoinduction with highly purified β-tricalcium phosphate in dog dorsal muscles and the proliferation of osteoclasts before heterotopic bone formation, Biomaterials 27 (25) (2006) 4419–4427.
[14] H. Yuan, C. Van Blitterswijk, K. De Groot, J. De Bruijn, A comparison of bone formation in biphasic calcium phosphate (BCP) and hydroxyapatite (HA) implanted in muscle and bone of dogs at different time periods, J. Biomed. Mater. Res. A 78 (1) (2006) 139–147.
[15] H. Yamasaki, H. Sakai, Osteogenic response to porous hydroxyapatite ceramics under the skin of dogs, Biomaterials 13 (5) (1992) 308–312.
[16] K. Kurashina, H. Kurita, Q. Wu, A. Ohtsuka, H. Kobayashi, Ectopic osteogenesis with biphasic ceramics of hydroxyapatite and tricalcium phosphate in rabbits, Biomaterials 23 (2) (2002) 407–412.
[17] H. Yuan, C.A. Van Blitterswijk, K. De Groot, J.D. De Bruijn, Cross-species comparison of ectopic bone formation in biphasic calcium phosphate (BCP) and hydroxyapatite (HA) scaffolds, Tiss. Eng. 12 (6) (2006) 1607–1615.
[18] L. Cheng, Y. Shi, F. Ye, H. Bu, Osteoinduction of calcium phosphate biomaterials in small animals, Mater. Sci. Eng.: C (2012).
[19] A. Barradas, H. Yuan, J. van der Stok, B. Le Quang, H. Fernandes, A. Chaterjea, M.C. Hogenes, K. Shultz, L.R. Donahue, C. van Blitterswijk, The influence of genetic factors on the osteoinductive potential of calcium phosphate ceramics in mice, Biomaterials 33 (23) (2012) 5696–5705.
[20] S. Fujibayashi, M. Neo, H.-M. Kim, T. Kokubo, T. Nakamura, Osteoinduction of porous bioactive titanium metal, Biomaterials 25 (3) (2004) 443–450.
[21] P. Habibovic, T.M. Sees, M.A. van den Doel, C.A. van Blitterswijk, K. de Groot, Osteoinduction by biomaterials—physicochemical and structural influences, J. Biomed. Mater. Res. A 77 (4) (2006) 747–762.
[22] G. Song, P. Habibovic, C. Bao, J. Hu, C.A. van Blitterswijk, H. Yuan, W. Chen, H.H. Xu, The homing of bone marrow MSCs to non-osseous sites for ectopic bone formation induced by osteoinductive calcium phosphate, Biomaterials 34 (9) (2013) 2167–2176.
[23] E.K. Yim, K.W. Leong, Significance of synthetic nanostructures in dictating cellular response, Nanomed.: Nanotechnol., Biol. Med. 1 (1) (2005) 10–21.
[24] M.J.P. Biggs, R.G. Richards, M.J. Dalby, Nanotopographical modification: a regulator of cellular function through focal adhesions, Nanomed.: Nanotechnol., Biol. Med. 6 (5) (2010) 619–633.
[25] R. Flemming, C. Murphy, G. Abrams, S. Goodman, P. Nealey, Effects of synthetic micro- and nano-structured surfaces on cell behavior, Biomaterials 20 (6) (1999) 573–588.
[26] E. Martinez, E. Engel, J. Planell, J. Samitier, Effects of artificial micro- and nano-structured surfaces on cell behaviour, Ann. Anat.—Anat. Anz. 191 (1) (2009) 126–135.
[27] A. Wood, Contact guidance on microfabricated substrata: the response of teleost fin mesenchyme cells to repeating topographical patterns, J. Cell Sci. 90 (4) (1988) 667–681.
[28] J. Meyle, K. Gültig, W. Nisch, Variation in contact guidance by human cells on a microstructured surface, J. Biomed. Mater. Res. 29 (1) (1995) 81–88.
[29] J.L. Charest, L.E. Bryant, A.J. Garcia, W.P. King, Hot embossing for micropatterned cell substrates, Biomaterials 25 (19) (2004) 4767–4775.
[30] C.C. Berry, G. Campbell, A. Spadiccino, M. Robertson, A.S. Curtis, The influence of microscale topography on fibroblast attachment and motility, Biomaterials 25 (26) (2004) 5781–5788.
[31] K.C. Popat, K.I. Chatvanichkul, G.L. Barnes, T.J. Latempa, C.A. Grimes, T.A. Desai, Osteogenic differentiation of marrow stromal cells cultured on nanoporous alumina surfaces, J. Biomed. Mater. Res. A 80 (4) (2007) 955–964.
[32] J.-P. Kaiser, A. Reinmann, A. Bruinink, The effect of topographic characteristics on cell migration velocity, Biomaterials 27 (30) (2006) 5230–5241.
[33] T.G. van Kooten, J.F. Whitesides, A.F. von Recum, Influence of silicone (PDMS) surface texture on human skin fibroblast proliferation as determined by cell cycle analysis, J. Biomed. Mater. Res. 43 (1) (1998) 1–14.
[34] M.J. Dalby, M.O. Riehle, S.J. Yarwood, C.D. Wilkinson, A.S. Curtis, Nucleus alignment and cell signaling in fibroblasts: response to a micro-grooved topography, Exp. Cell Res. 284 (2) (2003) 272–280.
[35] M.J. Dalby, N. Gadegaard, R. Tare, A. Andar, M.O. Riehle, P. Herzyk, C.D. Wilkinson, R.O. Oreffo, The control of human mesenchymal cell differentiation using nanoscale symmetry and disorder, Nat. Mater. 6 (12) (2007) 997–1003.
[36] A. Curtis, C. Wilkinson, Topographical control of cells, Biomaterials 18 (24) (1997) 1573–1583.
[37] R.G. Harrison, On the stereotropism of embryonic cells, Science 34 (1911) 279–281.
[38] A. Curtis, M. Varde, Control of cell behavior: topological factors, J. Natl. Cancer Inst. 33 (1) (1964) 15–26.
[39] K. Nakata, M. Umehara, T. Tsumura, Excimer laser ablation of sintered hydroxyapatite, Surf. Coat. Technol. 201 (9) (2007) 4943–4947.
[40] E. Stratakis, A. Ranella, M. Farsari, C. Fotakis, Laser-based micro/nanoengineering for biological applications, Prog. Quantum Electron. 33 (5) (2009) 127–163.
[41] H. Guo, J. Su, J. Wei, H. Kong, C. Liu, Biocompatibility and osteogenicity of degradable Ca-deficient hydroxyapatite scaffolds from calcium phosphate cement for bone tissue engineering, Acta Biomater. 5 (1) (2009) 268–278.
[42] M.F. Tabriz, P. Salehpoor, A.E. Kandjani, M. Vaezi, S. Sadrnezhaad, Particles size distribution effect on 3d packing of nanoparticles into a bounded region, Int. J. Eng. Trans. A Basics 20 (3) (2007) 281.
[43] M. Burdick, H. Parker, Effect of particle size on bulk density and strength properties of uranium dioxide specimens, J. Am. Ceram. Soc. 39 (5) (1956) 181–187.
[44] C.M. Kong, J.J. Lannutti, Effect of agglomerate size distribution on loose packing fraction, J. Am. Ceram. Soc. 83 (9) (2000) 2183–2188.
[45] A. Yu, N. Standish, L. Lu, Coal agglomeration and its effect on bulk density, Powder Technol. 82 (2) (1995) 177–189.
[46] D. He, N. Ekere, L. Cai, Computer simulation of random packing of unequal particles, Phys. Rev. E 60 (6) (1999) 7098.
[47] M. Sadat-Shojai, M.-T. Khorasani, E. Dinpanah-Khoshdargi, A. Jamshidi, Synthesis methods for nanosized hydroxyapatite of diverse structures, Acta Biomater. (2013).
[48] S.J. Kalita, A. Bhardwaj, H.A. Bhatt, Nanocrystalline calcium phosphate ceramics in biomedical engineering, Mater. Sci. Eng.: C 27 (3) (2007) 441–449.
[49] A. Wang, D. Liu, H. Yin, H. Wu, Y. Wada, M. Ren, T. Jiang, X. Cheng, Y. Xu, Size-controlled synthesis of hydroxyapatite nanorods by chemical precipitation in the presence of organic modifiers, Mater. Sci. Eng.: C 27 (4) (2007) 865–869.
[50] M. Descamps, L. Boilet, G. Moreau, A. Tricoteaux, J. Lu, A. Leriche, V. Lardot, F. Cambier, Processing and properties of biphasic calcium phosphates bioceramics obtained by pressureless sintering and hot isostatic pressing, J. Eur. Ceram. Soc. 33 (7) (2013) 1263–1270.
[51] I. Mobasherpour, M.S. Heshajin, A. Kazemzadeh, M. Zakeri, Synthesis of nanocrystalline hydroxyapatite by using precipitation method, J. Alloys Compd. 430 (1) (2007) 330–333.
[52] C. Liu, Y. Huang, W. Shen, J. Cui, Kinetics of hydroxyapatite precipitation at pH 10 to 11, Biomaterials 22 (4) (2001) 301–306.
[53] D. Bernache-Assollant, A. Ababou, E. Champion, M. Heughebaert, Sintering of calcium phosphate hydroxyapatite $Ca_{10}(PO_4)6(OH)_2$ I. Calcination and particle growth, J. Eur. Ceram. Soc. 23 (2) (2003) 229–241.
[54] G.J. Meijer, J.D. de Bruijn, R. Koole, C.A. van Blitterswijk, Cell based bone tissue engineering in jaw defects, Biomaterials 29 (21) (2008) 3053–3061.

[55] T. Safronova, V. Putlyaev, M. Shekhirev, Y. Tretyakov, A. Kuznetsov, A. Belyakov, Densification additives for hydroxyapatite ceramics, J. Eur. Ceram. Soc. 29 (10) (2009) 1925–1932.

[56] Z. He, J. Ma, C. Wang, Constitutive modeling of the densification and the grain growth of hydroxyapatite ceramics, Biomaterials 26 (14) (2005) 1613–1621.

[57] W. Suchanek, M. Yashima, M. Kakihana, M. Yoshimura, Hydroxyapatite ceramics with selected sintering additives, Biomaterials 18 (13) (1997) 923–933.

[58] S.M. Zakaria, S.H. Sharif Zein, M.R. Othman, F. Yang, J.A. Jansen, Nanophase hydroxyapatite as a biomaterial in advanced hard tissue engineering: a review, Tissue Eng. Part B: Rev. 19 (5) (2013) 431–441.

[59] A.C. Queiroz, J.D. Santos, R. Vilar, S. Eugénio, F.J. Monteiro, Laser surface modification of hydroxyapatite and glass-reinforced hydroxyapatite, Biomaterials 25 (19) (2004) 4607–4614.